

μ^+ charge exchange and muonium formation in low-pressure gases

Donald G. Fleming, Randall J. Mikula,* and David M. Garner
*Department of Chemistry and TRIUMF, University of British Columbia,
 Vancouver, British Columbia V6T 1Y6 Canada*

(Received 6 April 1982)

Using the basic muon-spin-rotation technique, the fractions of energetic positive muons thermalizing in diamagnetic environments (f_μ) or as the paramagnetic muonium atom (f_{Mu}) have been measured in low-pressure pure gases (He, Ne, Ar, Kr, Xe, H₂, N₂, NH₃, and CH₄) as well as in several gas mixtures (Ne-Xe, Ne-Ar, Ne-NH₃, and Ne-CH₄). In the pure gases, the muonium fractions f_{Mu} are generally found to be smaller than expected from analogous proton-charge-exchange studies, particularly in the molecular gases. This is probably due to hot-atom reactions of muonium following the charge-exchange regime. Comparisons with muonium formation in condensed matter as well as positronium formation in gases are also presented. In the gas mixtures, the addition of only a few hundred parts per million of a dopant gas (e.g., Xe) which is exothermic for muonium formation gives rise to an f_{Mu} characteristic of the pure dopant gas itself, demonstrating the importance of the neutralization process right down to thermal energies. In all cases, the experimental signal amplitudes are found to be strongly pressure dependent, which is interpreted in terms of the time spent by the muon as neutral muonium in the charge-exchange regime, $t_n < 0.2$ ns. This time is generally shorter in the case of molecular gases than in rare gases.

I. INTRODUCTION

Charge exchange is an important collision process relevant to understanding the behavior of plasmas and controlled fusion, the design of radiation detectors and studies of radiation damage. Although in recent years the focus of charge exchange has shifted to the study of multiply charged ions,^{1,2} it is still of interest to study the simplest charge-exchange process, that between a singly charged ion and an atom or molecule, particularly near thermal energies. The simplest ion is of course the proton and there have been a number of review articles in recent years on both the experimental results^{3,4} and theoretical calculations^{5,6} dealing with proton charge exchange. With the exception of a few reports of merged-beam⁷ and flowing-afterglow⁸ studies at or near thermal energies, most of the data on proton charge exchange has been provided by transmission experiments.^{3,4,9} In that type of study an energetic H⁺ (or H⁻) beam of typically ≥ 1 -keV energy (although data down to ~ 20 eV is available in selected cases⁴) is passed through a gas target at low pressure ($\sim 10^{-3}$ Torr), which is thin with respect to energy loss but thick with respect to charge equilibrium. Hence, by detecting the neutral

H atoms that pass through a magnetic field, for example, the cross section σ_{10} at energy E can be found. The fraction of H atoms produced at this energy can then be obtained from the ratio $\sigma_{10}/(\sigma_{10} + \sigma_{01})$, where σ_{10} and σ_{01} are the total cross sections for electron pickup and loss, respectively.

The positive muon (μ^+) has perhaps a more esoteric origin than the proton but its physical-chemical interactions with matter are identical to the proton's, except for any differences arising from their respective isotopic masses, $M_\mu = \frac{1}{9}M_p$. Muons are produced with kinetic energies of 4.1 MeV or greater, far larger than the energy regime of atomic interest. During its slowing down process in matter, the μ^+ undergoes charge exchange with molecules X of the medium, $\mu^+ + X \rightarrow (\mu^+e^-) + X^+$, in complete analogy with proton charge exchange. The neutral muonium atom (Mu) formed with cross section σ_{10} has as its nucleus a positive muon but otherwise can be regarded simply as a light isotope of the hydrogen atom.¹⁰⁻¹² The fraction of muons that thermalize in matter as either "free" μ^+ or as Mu atoms can easily be measured and interpreted in terms of well-established concepts in proton charge exchange.

There are three basic things to be learned from

the present study.

(1) Unlike the proton experiments, the μ^+ beam stops in the gas so that, in principle, one is able to probe the regime of charge exchange on the approach to thermal energies. In this regard, the information content is similar to that available from protons as thick target yields.

(2) The observable signal for the amount of muonium formed is a strong function of moderator pressure, which is interpretable in terms of the total time spent by the muon in the charge-exchange regime during its thermalization process. This time can be calculated theoretically^{9,13} but is otherwise difficult to obtain in proton experiments.

(3) The present results provide information on hot-atom processes which are of interest for comparison with similar studies in condensed media. Radiation chemistry spur processes may play a major role in the condensed phase^{14,15} but are expected to be unimportant in the gas phase.

The earliest study of muonium formation and muonium chemistry in gases was the work of Mobley *et al.*,¹⁶ using conventional "backward" muons of typically 125-MeV/c momentum, thereby necessitating the use of high-pressure (~ 40 -atm) targets. Later work by Stambaugh *et al.*¹⁷ and also by Barnett *et al.*¹⁸ concentrated on a study of muonium formation in gases, again using relatively high-energy muons and, in the case of Ref. 17, high-pressure targets. We have employed a surface muon beam^{19,20} which will easily stop in a gas like argon at ~ 1 -atm pressure. The present results, all obtained at the TRIUMF (Tri-University Meson Facility) cyclotron at the University of British Columbia, represent the first systematic study of μ^+ charge exchange and Mu formation in low-pressure gases. Preliminary reports primarily on the noble gases can be found in Refs. 21 and 22. More complete data are presented here including results for the polyatomic gases H_2 , N_2 , CH_4 , and NH_3 as well as results from gas mixtures.

II. EXPERIMENTAL

A. μ SR and MSR signals

Positive muons are produced with 100% longitudinal spin polarization,²³ which is maintained while the muon slows down until the onset of muonium formation during a series of charge-exchange cycles in the gas. The total slowing down time of the μ^+ /Mu ensemble (from ~ 2.5 MeV to 0.035 eV) is about 30 ns at 1-atm pressure in a gas-like argon.

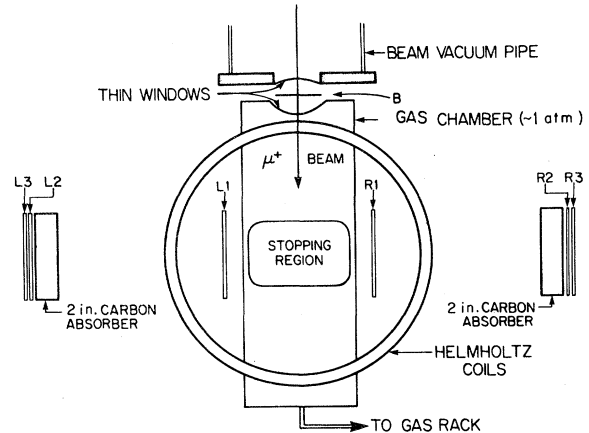


FIG. 1. Schematic diagram of the experimental apparatus. The μ^+ beam triggers the thin (B) counter and stops in the gas target, positioned between a pair of Helmholtz coils. Decay positions from $\mu^+ \rightarrow e^+ \nu_e \bar{\nu}_\mu$ are detected either in the "left" or "right" counter telescopes.

Much later, with a mean life $\tau_\mu = 2.2 \mu s$, the muon decays according to $\mu^+ \rightarrow e^+ \nu_e \bar{\nu}_\mu$ in which spatial parity is not conserved and the e^+ which is detected in the experiment exits preferentially along the muon spin direction.²³ A schematic diagram of the apparatus used is given in Fig. 1. A transverse magnetic field is provided by a pair of Helmholtz coils. A counter system fixed in the plane of muon spin precession (labeled "left" and "right" in Fig. 1) will exhibit an enhanced probability for detecting the decay positron each time the muon spin sweeps past.^{11,12,24-26} Hence a plot of the number of detected positrons $N(t)$ versus time shows oscillatory behavior. A typical example of a muon-spin-rotation (μ SR) spectrum is shown in Fig. 2 for muons in Ar gas at a pressure of 2.4 atm in a transverse magnetic field of 75 G, where the Larmor precession frequency of the muon, $\nu_\mu = 1.01$ MHz, cor-

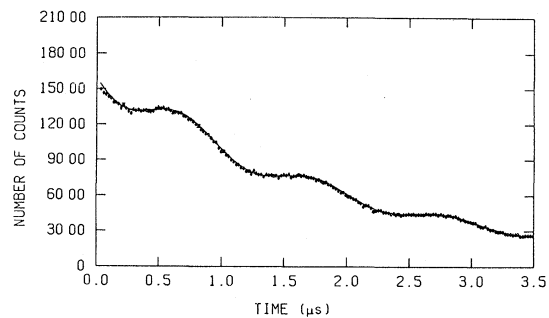


FIG. 2. Time histogram of muon precession in room-temperature Ar at 2.4 atm in a transverse magnetic field of 75 G. The curve is a χ^2 fit to the data.

responds to a precession period of 990 ns. In the case of the paramagnetic muonium atom, "triplet" Mu precesses in a weak transverse field 103 times faster than a diamagnetic muon, i.e., with half the electron's magnetic moment. Figure 3 gives the $N(t)$ spectrum for muonium spin rotation (MSR) in the same target as in Fig. 2 but at 8 G where the Mu Larmor frequency, $\nu_{\text{Mu}}=11.1$ MHz, corresponds to a precession period of 90 ns. Data of the type in Figs. 2 and 3 have the functional form

$$N(t) = N_0 e^{-t/\tau_\mu} [1 + S(t)] + B, \quad (1)$$

where N_0 is a normalization, $\tau_\mu = 2.197 \mu\text{s}$ is the muon lifetime, B is a time-independent background term, and $S(t)$ is the "signal" of interest, defined (in low fields) by

$$S(t) = A_{\text{Mu}} e^{-\lambda_{\text{Mu}} t} (\cos \omega_{\text{Mu}} t + \phi_{\text{Mu}}) + A_\mu e^{-\lambda_\mu t} (\cos \omega_\mu t - \phi_\mu), \quad (2)$$

where $A_\mu, \omega_\mu, \phi_\mu, \lambda_\mu$ and $A_{\text{Mu}}, \omega_{\text{Mu}}, \phi_{\text{Mu}}, \lambda_{\text{Mu}}$ are the amplitudes, frequencies, initial phases, and relaxation rates for the diamagnetic muon (Fig. 2) and muonium (Fig. 3) signals, respectively. In Eq. (2), the transverse relaxation rate $\lambda = 1/T_2$ is defined in analogy with nuclear magnetic resonance (NMR) or electron spin resonance (ESR) and corresponds to the spin-spin interaction of the muon or Mu with its environment. Sample MSR signals $S(t)$ are given in Fig. 4 for Mu precession in Kr gas at two pressures. The origin of the marked pressure dependence of the Mu amplitude (often called "asymmetry"), a general feature of all gases studied, is explained later. Similar results have been seen in Kr gas in a separate study at LAMPF (Los Alamos Meson Physics Facility).²⁷

The experiment consists of stopping a surface μ^+ beam (from the M20 channel of the TRIUMF cyclotron) in the gas target (Fig. 1), collecting a histo-

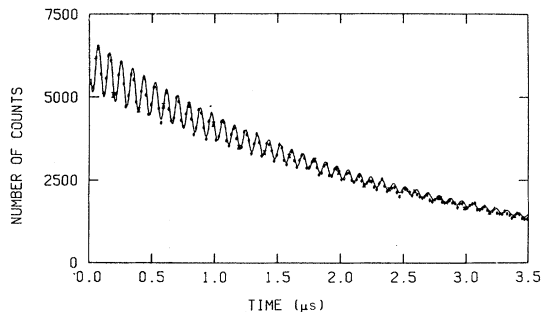


FIG. 3. Time histogram of muonium precession for the condition of Fig. 2 but in an 8-G applied field. The curve is a χ^2 fit.

gram of events in both the left and right telescopes, and separately fitting these to Eqs. (1) and (2) to yield the parameters of interest, principally A_{Mu} , A_μ , and λ . Often the relaxation of the MSR signal is the main focus of the experiment; λ_{Mu} may either be due to chemical reaction of the Mu atom^{10-12,24} or to spin exchange with paramagnetic molecules.^{13,28} The present study, however, focuses on the amplitudes A_μ and A_{Mu} since these are directly related to muonium formation in the gas; the relaxations λ_μ and λ_{Mu} in pure gases are dominated by field-inhomogeneity effects.¹³ The fraction of free muon f_μ and of muonium f_{Mu} thermalizing in the gas are related to the measured amplitudes A_μ and A_{Mu} by

$$f_\mu = \frac{A_\mu}{A_\mu + 2A_{\text{Mu}}}, \quad f_{\text{Mu}} = \frac{2A_{\text{Mu}}}{A_\mu + 2A_{\text{Mu}}}, \quad (3)$$

where the muonium amplitude has been multiplied by two to account for the unobserved antiparallel "singlet" fraction (classically, it does not precess). This nontrivial effect is treated in Sec. II B of the subsequent discussion. Defined in this way,

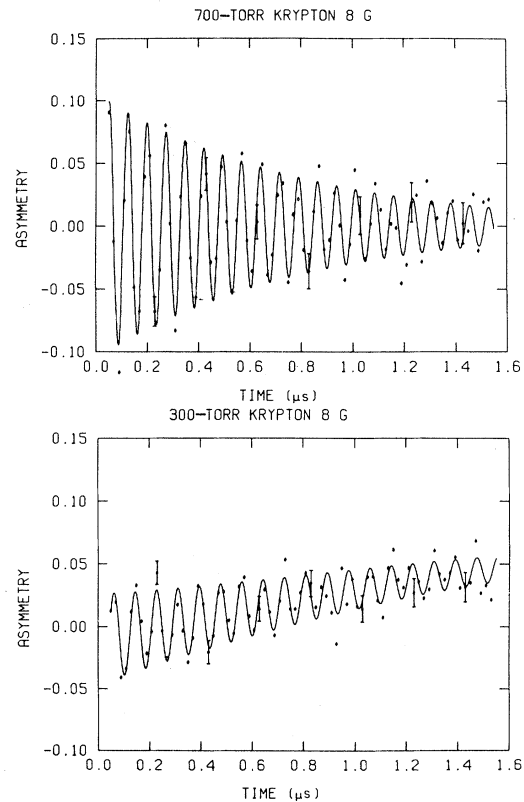


FIG. 4. The room temperature MSR amplitude in Kr gas in an 8-G field at a pressure of 700 Torr (top) and 300 Torr (bottom). The curves shown are χ^2 fits.

$f_{\text{Mu}} + f_{\mu} = 1$. The so-called free muon amplitude is in fact most likely due to the formation of μ^+ molecular ions. The evidence for this will not be discussed here but lies in the observation that the muon signal (λ_{μ}) relaxes noticeably upon the addition of a "reactive" dopant gas (e.g., Xe in Ne) due to *thermal* muonium formation.^{13,21} The neutral fraction f_{Mu} can be compared with the corresponding fraction f_{H} estimated from proton-charge-exchange cross sections.^{3,4} For the Ar data in Figs. 1 and 2, for example, $f_{\mu} = 0.28$ and $f_{\text{Mu}} = 0.72$; the fraction of thermal H atoms expected from proton data is 0.85.

Considerable care was taken with the purity of the noble gases, particularly He and Ne. These were purified by passing them over an activated-charcoal trap at liquid-nitrogen temperature or over a hot-titanium sponge or both. In general, hot titanium proved to be the most effective. One experiment with high-purity "research grade" Ne (99.99% purity; impurities are < 80 ppm He, < 15 ppm N₂, < 3 ppm O₂, H₂O, and < 2 ppm H₂) was also done in order to check the efficiency of the purification procedure. The polyatomic gases were not purified before use with the exception of H₂, which was passed through an activated-charcoal trap at liquid-nitrogen temperature.

B. μ^+ stopping distribution and wall effects

The mean range of a (4.1-MeV) surface μ^+ beam is ~ 135 mg/cm² (in Mylar) with a range spread determined largely by the momentum resolution of the channel.¹⁹ After traversing beam windows and defining counter, the residual range is ~ 80 mg/cm² with a spread of ~ 20 mg/cm² on the M20 channel at TRIUMF. This corresponds to a stopping distance of $\sim 40 \pm 15$ cm in a gas such as Ar at 1-atm pressure. The 75-cm-long gas target vessel was positioned near the center of a set of dual Helmholtz coils (Fig. 1) and the gas pressure adjusted to maximize the number of detected positrons.

Any muons initially scattered into the aluminum walls of the target vessel can affect the calculation of the formation fraction of muonium since such muons precess as free μ^+ with 100% of their initial polarization. It is important that these effects be understood and corrected for. In both the present work and the earlier work by Stambaugh *et al.*,¹⁷ it was found that almost all of the scattering was due to the beam defining counter(s) and target entrance window, with multiple scattering from the gas itself being negligible. In the present experiments the en-

trance window was thin Mylar or Kapton (0.012 cm) and the beam defining counter was 0.025 cm of NE-102 scintillator. At sufficiently high target gas pressures (e.g., ~ 2 -atm N₂) muons scattered from the entrance window are not able to reach the walls of the target vessel. This was determined using air as the target gas at different pressures. Since there is no muon or muonium signal in air itself, any signal can only come from the walls; e.g., at an air pressure of 0.4 atm, $A_{\mu} = 0.07 \pm 0.01$ but, at 1 atm, $A_{\mu} = 0.02 \pm 0.01$. Further corroborating experiments were done with a Mylar lining on the inside of the vessel; A_{μ} in Mylar is only 17% of that in Al. Since N₂ and air have essentially the same density, very accurate wall corrections could be made for N₂ but in general such corrections can only be extrapolated to other gases of widely differing densities and hence stopping distributions. Nevertheless, these can be made with some confidence and are duly recorded in the tables below. In the much higher pressure experiments of Stambaugh *et al.*,¹⁷ much thicker windows (0.6-cm Al) had to be used than in the present experiment. This causes severe scattering problems, which besides necessitating rigorous corrections to the data, reduces the useful signal.

C. Absolute asymmetries and solid-angle effects

The measured amplitudes of a typical μSR or MSR spectrum (e.g., Figs. 2–4) are dependent on a number of experimental variables: beam line optics, muon stopping distribution, counter geometry and solid angle, and, particularly, on the thickness of any accompanying degrader in the positron counters. This latter effect arises from the fact that the amplitude A_{μ} in $\mu^+ \rightarrow e^+ \nu_e \bar{\nu}_{\mu}$ decay [$A_{\mu} \sim 1 + a_{\mu}(E)\cos\theta$] is a strong function of energy as well as angle, obtaining its maximum value at 52.8 MeV when $\theta = 0$. The energy averaged value $\langle a_{\mu}(E) \rangle = \frac{1}{3}$.^{23,25,26} The surface μ^+ beam is accompanied by beam positrons of the same momentum (29 MeV/c), which give rise to random background events in the decay spectra. To effectively remove these positrons about 5 cm of carbon absorber was placed in front of the positron detectors (Fig. 1). As a result, the maximum amplitude in a given experiment is always empirically determined by a measurement of the $\mu^+\text{SR}$ spectrum in a target where no μ^+ depolarization occurs; an Al plate has been used in the present experiments. The *total absolute amplitude* can be defined by the fraction $A_{\text{abs}} = A_{\text{tot}}/A_{\text{Al}} = (A_{\mu} + 2A_{\text{Mu}})/A_{\text{Al}}$, where A_{μ} and A_{Mu} are the amplitudes in a given experiment and A_{Al} is the maximum amplitude possible, measured

under identical conditions. This ratio will always be ≤ 1 ; e.g., from Figs. 2 and 3, $A_{\text{abs}}=0.90$. It should be noted that any wall contributions to the observed muon amplitude A_{μ} (obs) must be corrected for.

The results of our experiments reveal a marked pressure dependence of the absolute amplitudes in all gases studied. As the later discussion will show, this pressure dependence (of the absolute asymmetries) is important in understanding the overall time dependence of muonium formation in the charge-exchange regime. This is not an effect of the muon stopping distribution on the solid angle for positron detection, as first suspected.²² Unlike experiments in condensed matter, where muons stop in a very well-defined region,^{12,14,15} the extended stopping distribution of the muon in the gas phase

may reduce the absolute signal amplitudes by phase averaging. Monte Carlo calculations have been carried out to simulate the muon stopping distribution and its random phase; for the counter geometry of our experiments the predicted effect was $\lesssim 10\%$. In addition, changing the experimental solid angle by a factor of 2 made only a few percent change in A_{μ} (obs). The maximum amplitude is always obtained with an Al plate in the center of the gas target vessel; spreading out the muon stopping distribution by placing 20-Al foils at intervals over a distance of 60 cm (target vessel length 75 cm) also causes only a 10% reduction in A_{μ} . We can thus unequivocally conclude that observed pressure-dependent amplitudes are due to the muon's slowing down process itself and not significantly to any geometrical effects.

TABLE I. Pressure-dependent μ^+ and Mu amplitudes in different gases.

Target Gas	Pressure (atm)	A_{μ} (obs) ^a	A_{μ} (walls) ^b	A_{Mu} ^a	A_{tot} ^c	$A_{\text{abs}}(\%)$ ^d
He	1.2	0.154±0.004	0.085	0.0	0.07	31
	2.7	0.210±0.003	0.070	0.0	0.13	48
	3.1	0.222±0.002	0.035	0.0	0.19	59
Ne	0.80	0.100±0.002	0.03	~0.02	0.11	28
	1.2	0.170±0.002 ^e	0.005	0.005±0.005 ^e	0.18	41
	1.6	0.255±0.003	0.015	0.015±0.005	0.27	62
	2.0	0.300±0.002	0.009	0.027±0.002	0.34	82
Ar	1.0	0.071±0.004	0.009	0.100±0.003	0.26	72
	2.0	0.092±0.003	0.005	0.111±0.004	0.31	85
	2.4	0.100±0.003	<0.005	0.130±0.004	0.36	90
	2.8	0.095±0.002	<0.005	0.143±0.003	0.38	96
Kr	0.40	0.065±0.004	0.065	0.040±0.004	0.08	32
	0.65	0.020±0.003	0.020	0.086±0.004	0.17	50
	0.95	0.020±0.003	0.020	0.120±0.006	0.24	68
Xe	0.40	0.046±0.003	0.046	0.050±0.003	0.10	36
	0.60	~0.04	~0.04	0.070±0.010	0.14	48
	0.65	0.040±0.010	0.040	0.089±0.006	0.18	58
H ₂	3.1	0.126±0.008	~0.02	0.086±0.008	0.28	82
N ₂	1.0	0.045±0.003	0.005	0.125±0.007	0.29	92
	2.4	0.076±0.002	<0.005	0.171±0.004	0.41	100
CH ₄	1.2	0.037±0.002	0.005	0.110±0.004	0.25	63
	3.0	0.058±0.002	<0.005	0.180±0.005	0.41	100
NH ₃	2.8	0.040±0.004	<0.005	0.182±0.003	0.40	100

^aExperimentally observed μ^+ and Mu amplitudes.

^bContribution to A_{μ} (obs) from walls at stated pressure.

^c $A_{\text{tot}}=A_{\mu}+2A_{\text{Mu}}$, where $A_{\mu}=A_{\mu}$ (obs)− A_{μ} (walls).

^d $A_{\text{abs}}=A_{\text{tot}}/A_{\text{Al}}$ for same experimental conditions.

^eObtained with research grade (99.99% Ne).

III. EXPERIMENTAL RESULTS

A. Pure gases

Results at different gas pressures for the measured amplitudes A_μ and A_{Mu} as well as the absolute total amplitudes are given in Table I. See also Fig. 4. It is to be noted that in Kr and Xe the measured muon amplitude is just the wall signal and hence one can conclude 100% Mu formation in these cases; just the opposite situation prevails in He and in Ne. Although the amplitudes are strongly pressure dependent, the relative fractions calculated from these amplitudes are not [Eq. (3)]. These pressure-independent fractions are given in Table II, along with the fractions similarly determined for the noble gases by Stambaugh *et al.* at much higher pressures.¹⁷ By and large the agreement is good, giving confidence in the method used to account for wall signal contributions [$A_\mu = A_\mu(\text{obs}) - A_\mu(\text{walls})$]. The Mu fractions f_{Mu} are also compared in Table II with expectations for H-atom formation from proton-charge-exchange studies^{3,4} extrapolated to thermal energies. Differences between f_{Mu} and f_{H} may be an indication of hot-atom reactions, as discussed further below.

The method used above to subtract the wall contribution from the observed muon amplitude is certainly the correct one in determining the *relative*

fractions since these can be identified with charge-exchange cross sections [see Eq. (4)] and hence should be pressure independent. However, there is some ambiguity in just how to best define the *absolute* amplitude A_{abs} , since this is markedly dependent on stopping pressure. One extreme is to subtract the wall contribution just as in defining the fractions themselves; this supposes that these μ^+ reach the walls before encountering any charge-exchange processes. The other extreme is to include the wall contribution and hence define A_{abs} in terms of $A_\mu(\text{obs})$; this supposes that these μ^+ strike the walls after (or during) the charge-exchange regime. The truth probably lies somewhere in between and we have elected to quote A_{abs} values in Table I (and following) as an average of these two extremes. In fact, this makes only an appreciable difference ($\pm 20\%$) in the case of low-pressure helium and neon, since the wall amplitudes are at the few-percent level in all other cases we have studied.

B. Muonium formation in doped rare gases

The study of muonium formation in gas mixtures is interesting in that it provides additional information on the mechanisms of charge exchange and perhaps also on hot-atom reactions. Previous studies of this nature have been carried out by Stam-

TABLE II. Relative fractions (in percent) of muonium (f_{Mu}) and of diamagnetic μ^+ (f_μ) found in different gases.

Target gas	Pressure or range in pressure (atm)	f_μ	f_{Mu}	f_{H}^b
He	1.2–3.1	100±1	0±1	15
	50 ^a	99±5	1±5	
Ne	1.2	93±5 ^c	7±5 ^c	20
	26 ^a	100±2	0±2	
Ar	1.0–2.8	26±4	74±4	85
	30 ^a	35±5	65±5	
Kr	0.4–0.95	0±5	100±5	100
Xe	0.4–0.65	0±4	100±4	100
	4.4 ^a	10±5	100	
H ₂	3.0	39±4	61±4	95
N ₂	1.0–2.4	16±4	84±4	90
NH ₃	2.8	9±4	91±4	100
CH ₄	1.2–3.0	13±4	87±4	100

^aHigher-pressure values from earlier study of Stambaugh *et al.*, Ref. 17.

^bExpected neutral fraction from proton-charge-exchange studies (Refs. 3 and 4).

^cTaken from the research grade Ne result of Table I which gives the most reliable μ^+ and Mu amplitude.

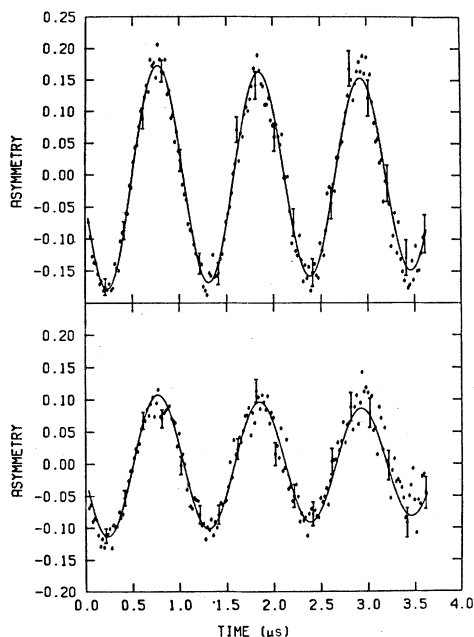


FIG. 5. The μ SR amplitude in pure Ne at room temperature in a 70-G magnetic field at 1.2 atm (top) and with 200 ppm of added Xe (bottom). The curves shown are χ^2 fits.

baugh *et al.*, but again at relatively high moderator pressures in He and Ne and only at two different partial pressures of added Xe.¹⁷ In the present study Ne was chosen preferentially as an inert moderator since it has essentially no muonium formation (Table II) and, unlike helium, it provides a good muon stopping density at low pressures. Complete studies (up to five different partial pres-

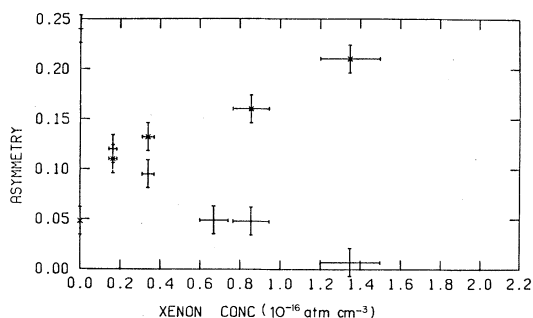


FIG. 6. A plot of the μ SR and MSR amplitudes, A_μ (corrected for walls) and $2A_{Mu}$ (indicated by *) as a function of added dopant Xe concentration in 1.2-atm Ne at room temperature. The vertical error bars shown are the results of χ^2 fits to the data and are 1σ errors. The horizontal bars are estimates of uncertainties in the added Xe concentrations. Note the initial value at zero Xe concentration.

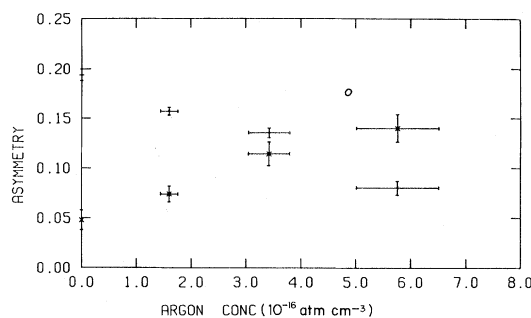


FIG. 7. As in Fig. 6, but for added Ar.

ures) were carried out for Ne doped with Ar, Xe, CH_4 , and NH_3 . Partial results were also obtained for Xe and NH_3 in He. Figure 5 shows the effect of adding trace amount of dopant gas on the experimental signal; the μ SR signal in pure Ne (top, 1.2 atm) is markedly reduced in amplitude upon the addition of 0.19-Torr Xe (200 ppm). The same effect is seen with the addition of Ar although in this case much more is required since muonium formation is not an exothermic process in collisions with Ar. The loss of amplitude of the muon signal (and corresponding enhancement of muonium) is attributed to epithermal muonium formation. The amplitudes A_{Mu} and A_μ are plotted as a function of added dopant concentration for Xe added to Ne (Ne-Xe), Ar added to Ne (Ne-Ar), CH_4 added to Ne (Ne- CH_4), and NH_3 added to Ne (Ne- NH_3) in Figs. 6–9, respectively; Xe, NH_3 , and CH_4 are all exothermic for Mu formation. It can be seen that, within errors, the total asymmetry is constant. This is confirmation that muonium formation in these systems is an epithermal process, even though it is energetically allowed at thermal energies for Xe (and for CH_4 and NH_3). If it were a thermal process, muonium formation would occur at random times leading to no coherence and hence no observable Mu precession. Note the difference in the high-concentration asymptotes. In the case of Ne-

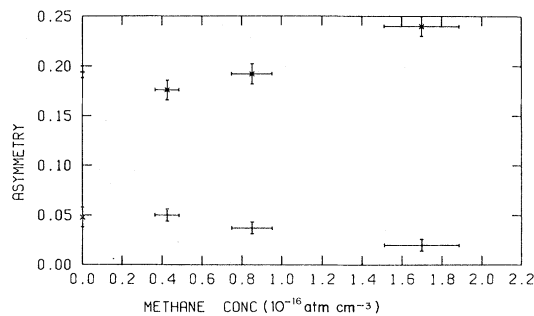


FIG. 8. As in Fig. 6, but for added CH_4 .

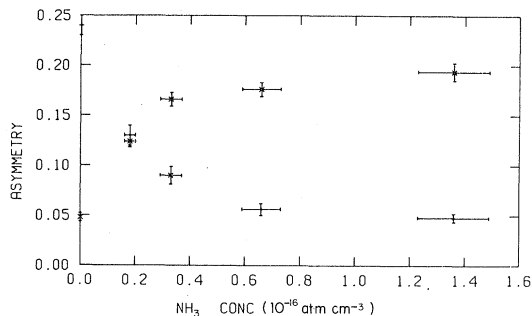


FIG. 9. As in Fig. 6, but for added NH₃.

Xe mixtures (Fig. 6), there is 100% Mu formation in Xe and hence (within errors) the μ^+ signal goes to zero at high enough Xe concentrations. On the other hand, in the cases of Ne-Ar (Fig. 7), Ne-CH₄ (Fig. 8), and Ne-NH₃ (Fig. 9) mixtures, the muon signal is asymptotic to the fraction seen in the pure dopant gases (Table II); this is particularly noticeable in the case of Ar in Ne. It might also be pointed out that if there were an appreciable residual wall signal in these data, then all muon signals would be asymptotic to the same value.

In gas mixtures such as Ne-Xe, Ne-NH₃, or Ne-CH₄, for which the ionization potential of the added gas is lower than that of muonium itself (13.6 eV), one expects large formation cross sections ($\sigma_{10} \geq 10^{-15}$ cm²) at low energies, at the end of the charge-exchange regime. Thus, e.g., in Figs. 6, 8, and 9, Mu formation typical of the pure dopant is seen at a concentration of only 500 ppm in neon. In a helium moderator the effect is qualitatively the same although it takes relatively more Xe or NH₃ in He than in a Ne moderator. This is a reflection of the enhanced moderator efficiency of He compared to neon. The same effect had been seen in the earlier study of Ref. 17. The level of sensitivity seen at small concentrations of some dopant "impurity" gas necessitates special care in purifying He and Ne in order to obtain the optimum signal in these gases. When the dopant gas has a higher ionization potential than muonium, the rise of f_{Mu} as a function of concentration is more gradual. This is dramatically illustrated in the case of argon in neon in Fig. 7, where complete muonium formation requires much larger concentrations than in the case of xenon. This difference is a reflection of the fact that the electron-capture cross sections of low energy μ^+ in argon are much smaller than in xenon (or in ammonia or methane) and are comparable to those in neon itself.

IV. DISCUSSION

A. Primer on muon (proton) charge exchange

Muonium can simply be regarded as an isotope of hydrogen and hence Mu formation in gases can generally be understood in terms of well-established concepts of proton charge exchange.³⁻⁹ As a muon (proton) thermalizes in a gas it passes through three broad regimes of energy loss. The first is at high energies where the muon loses most of its initial energy (after traversing beam line windows and plastic scintillator, see Fig. 1) of ≥ 2.5 MeV through Bethe-Bloch-type ionization of the material it is slowing down in. During this process no appreciable amount of muonium forms. This process dominates until μ^+ energies of about 35 keV are reached. At this energy the muon velocity is comparable to the outer orbital electron velocities of the moderator (cf. ~ 300 keV for protons), defining then the onset of Mu formation through a series of electron capture and loss cycles. In this second regime, from about 35 keV to about 50 eV (or ~ 450 eV for protons), the muon undergoes a series of charge-exchange cycles, $\mu^+ + e^- \rightleftharpoons \text{Mu}$, spending an appreciable amount of its time as a muonium atom and ultimately emerging as either diamagnetic muon or as muonium. In this regime, the cross section for muonium formation (σ_{10}) is expected to peak at an energy given by the "adiabatic criterion" introduced by Massey.²⁹ This energy is about 150 eV for the μ^+ in a gas such as Ar or N₂ (cf. 1.3 keV for the proton or about 4.0 keV for the triton). When the muon is at a low enough energy (≤ 50 eV), charge exchange no longer happens and the μ^+ or the Mu atom enters the third regime where thermalization occurs via elastic and inelastic collisions.

For an incident beam of +1 charge (muon or proton), the fractions of neutral (f_0) and charged (f_1) species formed at energy E in the gas can be represented by

$$f_1(E) = f_\mu = \frac{\sigma_{01}}{\sigma_{01} + \sigma_{10}} \quad (4)$$

and

$$f_0(E) = f_{\text{Mu}} = \frac{\sigma_{10}}{\sigma_{01} + \sigma_{10}},$$

where σ_{10} and σ_{01} are the cross sections for electron capture and loss, respectively. In Eqs. (4) one expects the muon and proton fractions to be the same at energy $E_\mu = \frac{1}{9} E_p$; i.e., equal cross sections at equal velocities. This simple scaling is certainly justified at proton energies of ≥ 100 keV and Born ap-

proximation calculations agree well with the classical Thomas model for charge exchange in this energy region.^{5,6,30,31} Even at lower energies (~ 1 -keV protons) charge-exchange cross sections are expected to be mass independent although with considerably different velocity dependences than seen at higher energies.^{29,32} It is not so clear, however, just how low in energy one can expect strictly velocity-dependent charge-exchange cross sections to be operative. In this regard, the μ^+ data provides a useful complement to the proton since it actually stops in the gas, thereby probing charge exchange right down to thermal energies. The fractions of neutral muonium expected based on the corresponding H atom fractions f_H have been given in Table II.

It should be noted that the present experiments, and also with rare exceptions³³ the proton transmission experiments with which they are compared, do not distinguish electron pickup from different shells nor is ground-state capture distinguishable from capture to excited atomic states ($n > 1$). In general, though, Mu formation should be dominated by outer-shell electron capture at the energies of interest³⁴ and capture to excited states is expected to be a small effect, scaling by about $1/n^3$.³⁵

It is convenient to divide the total slowing-down time of the μ^+ in the gas also into three time domains, corresponding to the different energy domains mentioned above. In the high-energy Bethe-Bloch domain where ionization processes dominate, proton stopping powers are well known³⁶ so that the time " t_1 " can be straightforwardly calculated for the μ^+ to slow down to say 35 keV (300 keV equivalent proton velocity). For example, in

Ar at 1-atm pressure, $t_1 = 14$ ns (inversely dependent on the electron density and the pressure of the gas). At about 35 keV, the μ^+ enters the charge-exchange domain losing a minimum energy in each cycle essentially equivalent to the ionization potential of the moderator. The time " t_n " spent as a neutral in this second regime can be conveniently expressed as⁹

$$t_n = \frac{P_0 T}{P T_0} \int_{E_i}^{E_f} f_0(E) \frac{1}{v_p} \left[\frac{dE}{dx} \right]^{-1} dE, \quad (5)$$

where P_0 is 1 atm, T_0 is 273 K, $v_p(E)$ is the speed of the particle at energy E , and $f_0(E)$ is the neutral fraction at that energy [Eq. (4)]. This time depends simply upon the pressure and temperature of the target gas and has an asymptotic behavior dependent upon the lower-energy limit E_f . In general both dE/dx and cross-section data for protons are well known only down to about 9 keV (1-keV μ^+) and this limit for E_f is then taken for the purpose of comparison between different gases. These calculated times are given in Table III at representative pressures for those gases where complete dE/dx data is available. The total time taken in this regime, " t_2 ," will not be weighted by $f_0(E)$ in Eq. (5) and hence will be greater than t_n itself, typically by about a factor of 3, yielding a total time t_2 of order 0.1 ns.⁹

The number of charge-changing cycles N_c is an integral over the corresponding stopping cross sections, rising rapidly as the muon (proton) slows down from high energies and then asymptotically leveling off at low energies.^{9,13,17} Results for H₂, N₂, and the noble gases assuming an initial energy of 35 keV and a final energy of 1-keV μ^+ (extend-

TABLE III. Number of charge-changing cycles and slowing-down times for the μ^+ in gases.

Gas	N_c^a	Pressure (atm)	$t_1(ns)^b$	$t_n(ns)^c$	$t_3(ns)^d$
He	111	3.1	30	0.077	0.63
Ne	53	1.2	18	no data	8.2
Ar	76	1.0	14	0.014	19.1
Kr	95	0.8	10	0.014	50.2
Xe	no data	0.6	11	$\leq .014^e$	101
H ₂	71	3.1	30	0.043	0.32
N ₂	77	1.0	18	0.030	13.4

^a $E_i > 35$ keV, $E_f = 1$ keV, except in case of Ne where available proton data extends down only to an equivalent 4.4-keV μ^+ energy.

^bBethe-Bloch ionization, from 3 MeV to 35 keV.

^cTime spent as neutral during the charge-exchange regime, from 35 to 1 keV. The actual total time t_2 spent in this region would be a factor of 2–3 longer.

^dFinal thermalization time from 50 eV to 0.035 eV (300 K) assuming elastic collisions only and an energy-independent cross section of 10^{-15} cm².

^eComplete data not available, but t_n expected to be less than in Kr.

ing this to lower energies has little effect) are also given in Table III. On average, we see that the μ^+ undergoes about 80 charge/changing cycles. The actual energy at which no further charge exchange occurs is not well established, but can be estimated from the condition $(dN_c/dE)E \leq 1$, using extrapolated proton ranges and cross sections; e.g., in Ar $(dN_c/dE) \sim 0.03 \text{ eV}^{-1}$ at 30 eV while in He it is $\sim 0.01 \text{ eV}^{-1}$ at 90 eV. Thus, for the muon, at about 50 eV on average no further *cyclic* charge exchange is expected which means that the muon emerges from a series of charge-exchange cycles at this energy as either a diamagnetic muon or Mu. It is to be noted then that stable muonium forms at fairly low energies in the gas; the corresponding energy for the proton would be $\sim 450 \text{ eV}$ and for the triton $\sim 1400 \text{ eV}$, depending on the moderator. It is in this energy region down to near thermal energies, where hot-atom/ion reactions may be important, as referred to again in the subsequent discussion. For the purpose of the later discussion, it is also worth noting here that if the integral in Eq. (5) is extended down to $E_f \sim 50 \text{ eV}$, then $t_n \sim 0.08 \text{ ns}$ at 1-atm pressure in a reasonably dense gas such as Ar or N_2 .

In the third and final energy-time regime down to $E_f = \frac{3}{2}k_B T$, the remaining energy loss is expected to be primarily by elastic collisions, at least for the rare gases. Assuming an average scattering angle of 90° , one obtains for the integrated time " t_3 ,"

$$t_3 = \frac{M}{\sqrt{2}m n \sigma} \left[\frac{1}{E_f^{1/2}} - \frac{1}{E_i^{1/2}} \right], \quad (6)$$

where M is the mass of the moderator gas of density n (atoms/cm³), m the mass of the stopping particle, and σ is some effective cross section. As expected, the heavier the moderator gas, the less efficient it is in thermalizing the muons by elastic collisions. The same effect contributes in the charge-exchange regime as well. These times are also compared for the rare gases in Table III, assuming $E_i = 50 \text{ eV}$ and $E_f = 0.035 \text{ eV}$ (300 K) and with an (energy-independent) cross section of 10^{-15} cm^2 . This value is typical for H-atom elastic scattering on light atoms or molecules at fairly low energies.^{29,37}

Finally, it must be emphasized that there are no clear-cut boundaries to the energy regimes in the slowing-down process and that the overlap, especially of the charge-changing and elastic-collision thermalization processes, is vital to the understanding of the final muonium-formation fractions and asymmetries in various gases. The total slowing-down time $t_1 + t_2 + t_3$ from Table III is of order 30

ns in a gas such as Ar at 1-atm pressure; the inclusion of inelastic processes in molecular gases (see, e.g., Ref. 38) as well as the possibility of electronic excitation at higher energies, may serve to make these times considerably shorter. Detailed calculations of the type carried out by Mozumder³⁹ for electron thermalization times, but including inelastic collisions, would be extremely valuable. It is of interest to note that the fastest time the muon can slow down is given by \bar{R}/v_i , where \bar{R} is the mean range in the gas and v_i the initial velocity. For example, in 1-atm Ar this time is about 10 ns; in condensed matter it would be about 0.01 ns.

B. Observed amplitude for muonium

The marked pressure dependence seen in the μ^+ /Mu amplitudes of Table I—typically a factor of 2 or 3 for the same change in pressure—is a result of Mu formation and concomitant muon depolarization during the charge-exchange regime. Consequently, the time scale for this process must be comparable to the time scale for neutralization in the charge-exchange regime.

1. Time dependence of the μ^+ polarization

Since the μ^+ is initially 100% spin polarized (α_μ) but the captured electron is not, muonium forms initially in parallel ($|\alpha_\mu\alpha_e\rangle$) and antiparallel ($|\alpha_\mu\beta_e\rangle$) states with equal probability. In zero or weak longitudinal magnetic fields, the parallel (triplet) state is an eigenstate of the isotropic Hamiltonian:

$$H = g_e\beta_e\vec{S}_e \cdot \vec{B} - g_\mu\beta_\mu\vec{I}_\mu \cdot \vec{B} + A\vec{S}_e \cdot \vec{I}_\mu. \quad (7)$$

The field-dependent eigenvalues for muonium are given in the familiar Breit-Rabi diagram in Fig. 10. The antiparallel state is not, however, an eigenstate, oscillating instead between $|\alpha_\mu\beta_e\rangle = (1/\sqrt{2})[|10\rangle + |00\rangle]$ and $|\beta_\mu\alpha_e\rangle = (1/\sqrt{2})[|10\rangle - |00\rangle]$ at the hyperfine frequency $A/h = \nu_0 = 4463.3 \text{ MHz}$ ($|FM_F\rangle$ represent the usual hyperfine-coupled quantum numbers). Consequently, the formation of antiparallel (singlet) muonium for sufficiently long times effectively depolarizes the positive muon, since experimental time resolutions are typically $\sim 1 \text{ ns}$, much longer than $1/\nu_0 = 0.22 \text{ ns}$.

In a transverse magnetic field (with respect to the μ^+ spin), neither the parallel nor antiparallel states are eigenstates but these can be expressed in terms of the eigenstates of the Hamiltonian by a suitable transformation.^{11,24-26} The time and field depen-

dence of the μ^+ polarization in muonium then has the form

$$P_\mu(t) = \frac{1}{4} [(1+\delta)(e^{i\omega_{12}t} + e^{-i\omega_{34}t}) + (1-\delta)(e^{i\omega_{23}t} + e^{i\omega_{14}t})], \quad (8)$$

where the ω_{ij} 's ($\omega = 2\pi\nu$) are defined in Fig. 10 and $\delta = X/(1+X^2)^{1/2}$; X is the dimensionless ratio H/H_0 , where H is the applied field and $H_0 = 1585$ G is the contact field of the μ^+ at the electron (cf. 503 G for the H atom). In moderate magnetic fields, $H \lesssim 200$ G, δ is approximately zero and there are four allowed ($\Delta M = \pm 1$) transition frequencies; but, both ν_{14} and ν_{34} are comparable to ν_0 (4463 MHz) and hence are not resolvable with the 1 ns (or longer) time resolution of a typical μ SR experiment. Consequently, only the frequencies ν_{12} and ν_{23} are seen. From Eq. (8), the real part of the time dependence of the muon polarization in muonium in moderately weak magnetic fields can be written approximately in the form

$$\text{Re}P_\mu(t) \approx \frac{1}{2} \cos\omega_{\text{Mu}}t [\cos\Omega t + \cos(\omega_0 + \Omega)t], \quad (9)$$

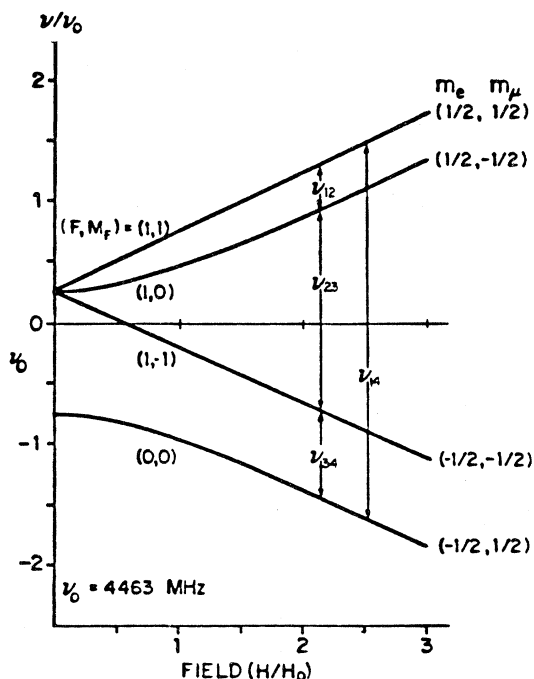


FIG. 10. Breit-Rabi diagram as a function of the dimensionless quantity H/H_0 ($H_0 = 1586$ G) showing the energy levels of muonium in a magnetic field. The allowed transition (precession) frequencies in a transverse field are indicated. In weak fields ($\lesssim 10$ G), ν_{12} and ν_{23} are degenerate, leading to characteristic coherent muonium precession.

where $\omega_{\text{Mu}} = 2\pi\nu_{\text{Mu}}$ is the radial frequency of coherent Mu, $\omega_0 = 2\pi\nu_0$ is the Mu hyperfine frequency (2.8×10^{10} rad s $^{-1}$), and $\Omega \approx \omega_{\text{Mu}}^2/\omega_0$ is a "beat frequency" characteristic of two-frequency muonium precession.^{24-26,40} The first term of Eq. (9) can be identified with the original parallel fraction ($\alpha_\mu\alpha_e$) of muonium formed and the second term with the original antiparallel fraction ($\alpha_\mu\beta_e$). In magnetic fields of interest, $\omega_0 \gg \omega_{\text{Mu}} \gg \Omega$ and the second term of Eq. (9) averages to zero at observation times and hence is responsible for depolarization of half of the muon ensemble. This is the situation in the third and final stage of thermalization, where slowing-down times are of order 10 ns (Table III). This situation is made clearer with reference to Fig. 11 which presents the exact dependence represented by Eq. (8) at very early times in a field of 100 G; the approximate form of Eq. (9) yields virtually the same result on this time scale. The fast oscillations in Fig. 11 are due to $1/\nu_0$ (0.22 ns), while the slow modulation is essentially due to $1/\nu_{\text{Mu}}$ (7.1 ns at 100 G). The fast oscillations are not observed in the experiment. In weak magnetic fields, $B \lesssim 10$ G, $\Omega \rightarrow 0$ (ν_{12} and ν_{23} become degenerate, Fig. 10) giving rise to the Larmor precession frequency of triplet muonium, $\nu_{\text{Mu}} = 1.39B(\text{G})$ MHz. This is the basic form of the MSR signal described earlier [Eq. (2), Figs. 3 and 4]. Classically, the loss of so-called singlet muonium can be identified with its zero spin and hence zero precession in the applied field [recall also Eq. (3)].

2. Pressure-dependent muonium formation

At the other end of the time scale, at very early times, only the second term of Eq. (9) and, indeed, just its $\cos\omega_0 t$ dependence will be important. In particular, singlet Mu formed in the charge-

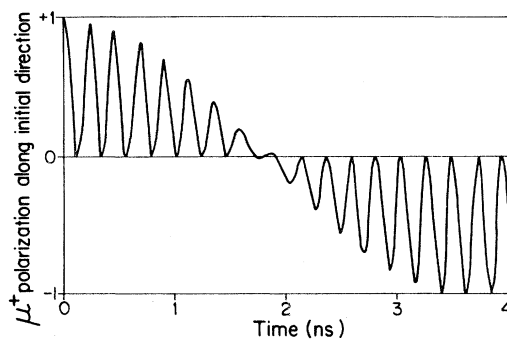


FIG. 11. Time evolution of the real part of the μ^+ polarization in free Mu in a 100-G transverse field. The fast oscillations at the hyperfine frequency $\nu_0 = 4463.3$ MHz are not observed experimentally.

exchange regime for a time sufficiently long for the μ^+e^- hyperfine interaction to mix states will cause additional loss of muon polarization. This situation can again be appreciated with reference to Fig. 11 but for a time regime compressed by about a factor of 10. The question of relevance here is how many charge-exchange cycles are important in determining the final μ^+ or Mu polarization? In total, there are something like 80 charge-exchange cycles as the muon slows from 35 to 1 keV in a time ~ 0.05 ns (Table III). Thus, on average, the time per cycle is ~ 0.6 ps, $\ll 1/\nu_0$, and hence far too short to ac-

count for any depolarization of the muon. On the other hand, the time per cycle will certainly be longer at the lower-energy end of the charge-exchange domain. Moreover, the energy regime where charge-exchange cycles are important extends down to well below 100 eV and probably down to 20 or 30 eV in those moderators for which Mu formation is an exothermic process. It will only be the last few cycles (perhaps only the very last cycle) which determines the μ^+ or Mu amplitude. Lacking detailed knowledge on how to calculate the correct correlation time for this muon depolariza-

TABLE IV. Total muon (pressure-dependent) amplitudes and singlet depolarization times, t_s .

Gas	Pressure (atm)	A_{abs} (%) ^a	t_s (ns) ^b	$A_{\text{predicted}}$ ^c	t_n (ns) ^d
He	1.2	31	0.15	— ^f	0.30
	2.7	48	0.068	50	0.14
	3.1	59	0.060 ^e	59 ^e	0.12
Ne	0.8	28	0.095	17	0.19
	1.2	41	0.063	56	0.12
	1.6	62	0.048	72	0.10
	2.0	82	0.038 ^e	82 ^e	0.076
Ar	1.0	72	0.044	76	0.088
	2.0	85	0.022	93	0.044
	2.4	90	0.018	95	0.036
	2.8	96	0.016 ^e	96 ^e	0.032
Kr	0.40	32	0.12 ^e	— ^f	0.24
	0.65	50	0.073	44	0.15
	0.95	68	0.052 ^e	68 ^e	0.10
Xe	0.40	36	0.10 ^e	12 ^{e,f}	0.20
	0.60	48	0.068	50	0.14
	0.65	58	0.061 ^e	58 ^e	0.12
H ₂	3.1	82	0.037 ^e	82 ^e	0.074
N ₂	1.0	92	0.025 ^e	92 ^e	0.050
	2.4	100	0.010	99	0.020
CH ₄	1.2	63	0.057 ^e	63 ^e	0.11
	3.0	100	$\leq 0.01^{e,f}$	$\geq 99^{e,f}$	< 0.02
NH ₃	2.8	100	≤ 0.01	$\geq 99^{e,f}$	< 0.02

^aTotal absolute amplitudes from Table I.

^bCalculated from Eq. (10), normalizing in each case to a given pressure and observed amplitude and then calculating t_s from a ratio of pressures.

^cUsing the calculated times t_s and Eq. (10).

^dTotal Mu neutralization time assumed to be twice t_s .

^eNormalized value of A_{abs} and hence calculated t_s .

^fEither pressure too low or A_{abs} 100% and so calculation is not meaningful; hence as in footnote e.

tion, we will assume it can be represented by a time " t_s " as an average of $\cos\omega_0 t$ over the time interval spent in the singlet Mu state:

$$\langle \cos\omega_0 t \rangle = \frac{\sin\omega_0 t}{\omega_0 t}. \quad (10)$$

As long as this time is small, there is little or no depolarization; e.g., if $t_s = 10^{-11}$ s, $\cos\omega_0 t = 0.98$ and essentially all of the polarization is retained. This is approximately the case for 2.8-atm Ar where A_{abs} is 96%, from which one can estimate $t_s = 1.6 \times 10^{-11}$ s. Since this time is inversely proportional to pressure, it can be predicted that at 1-atm pressure t_s should be 4.4×10^{-11} s and hence A_{abs} at 1 atm should be 76%, in good agreement with the experimental value. It is assumed that those muons in triplet Mu retain their full polarization and hence the total time t_n spent as a neutral should be just twice t_s . Table IV shows these estimated times and predicted A_{abs} for the data from Table I and the agreement is satisfactory, considering the simplicity inherent in the model—the trends in each case are well reproduced. It is probable that, at very low pressures, the argument of $\sin\omega_0 t$ changes too rapidly to be meaningful. Nevertheless, this type of estimate is useful although it would clearly be desirable to have detailed theoretical calculations of the appropriate correlation time along the lines calculated in Ref. 41. In general, though, it can be concluded that the time spent as a neutral ($t_n = 2t_s$) in the charge-exchange regime varies from about 0.02 to about 0.20 ns, depending primarily on the gas-pressure charge density. Such information cannot be obtained from proton-charge-exchange data. These estimates are invariably larger than the calculations reported in Table III based on proton data down to 1-keV muon energy but are consistent with an evaluation of the integral in Eq. (5) using extrapolated proton data down to a lower-energy limit of 50 eV.

It is clear that the slowing-down times in the charge-exchange regime are of sufficient magnitude to significantly depolarize the muon, particularly at pressures lower than 1 atm. This conclusion is in contrast to initial speculation.^{24,25} It should be noted that the level of paramagnetic impurities in the gas (e.g., O_2) is negligibly small so that electron spin exchange cannot be a source of μ^+ depolarization.²⁸ As mentioned already, it must be only the last few charge-exchange cycles where depolarization occurs and correspondingly it is the accompanying cross sections at low energy which are most important in determining the amount of polarized muonium formed.

Supporting evidence for this comes from measurements in doped rare gases (Figs. 6, 8, and 9); the addition of low ionization potential (< 13.6 eV) dopants at the 100-ppm level can only be effective if there is a relatively long time between collisions, thereby enhancing the probability of the muon finding a Xe atom in a bath of Ne atoms for example. This process occurs *after* the μ^+ or Mu has passed through the charge exchange regime with the Ne bath; i.e., at energies $\lesssim 50$ eV. At these energies the μ^+ or Mu probably undergoes several elastic and inelastic collisions which do not involve charge exchange (with the added Xe) and the time between successive charge-exchange collisions increases. A quantitative calculation of this time and/or of the cross section involved is not easy to arrive at but a rough estimate can be made. The data exhibit an exponential dependence of the muon amplitude on the concentration of added dopant (e.g., Ne-Xe in Fig. 6). This is expected since the change in amplitude A_μ in path length x as the muon slows down in the gas can be interpreted in terms of an attenuation law which for the present case of thick-target yields can be approximated by the form

$$A_{\mu^+} = A_0 e^{-n\sigma x} = A_0 e^{-n\sigma \bar{v}t}, \quad (11)$$

where A_0 is the muon amplitude in the absence of added Xe (of concentration n), σ is some effective cross section, and \bar{v} is an appropriate average velocity to travel the length x during time t . In principle, the amplitude of Eq. (11) should be written as a function of the path length x and the thick-target yield expressed as an integral result, $A_\mu(\text{obs}) = \int A_\mu(x) dx$; lacking detailed knowledge of this though we replace x by its average $\bar{x} = \bar{v}t$ where t is the total thermalization time in the energy interval ΔE from ~ 50 eV to thermal energies. In this energy regime, $\sigma_{10} \gg \sigma_{01}$ so that the cross section of Eq. (11) should be just σ_{10} for the collision process $\mu^+ + \text{Xe} \rightarrow \text{Mu} + \text{Xe}^+$. In a Ne moderator, if the thermalization time t_3 of 8.2 ns is taken from Table III, then \bar{v} in this interval is 1.9×10^7 cm s⁻¹ and σ is found to be 1.7×10^{-15} cm²/atom. This is in qualitative agreement with expected values of σ_{10} for H-atom formation in Xe at low energies, particularly in view of the large uncertainties reported in the proton data.^{3,4}

Table V compares the muon amplitudes A_{abs} for different gases in relation to both the number density and charge density of these gases, assuming it is only the "valence" electrons that are important. This is consistent with the energetics and cross sections discussed earlier. (A slightly more sophisticat-

TABLE V. Muon amplitudes and densities for gases.

Gas	Pressure (atm)	$\rho(g/l)^a$	$\rho_e(\bar{e}/cm^3 \times 10^{20})^b$	$A_{abs}(\%)^c$	$t_n(ns)^c$
He	1.2	0.22 (0.33)	0.66	31	0.30
H ₂	3.1	0.24 (0.72)	1.4	82	0.074
Ne	0.80	0.65 (0.20)	1.6	28	0.19
He	3.1	0.55 (0.83)	1.7	59	0.12
Kr	0.40	1.4 (0.10)	1.8	32	0.24
Xe	0.40	2.1 (0.10)	1.8	36	0.20
Ar	1.0	1.6 (0.24)	2.0	72	0.088
N ₂	1.0	1.1 (0.24)	2.4	92	0.050
CH ₄	1.2	0.78 (0.30)	2.4	63	0.11
Xe	0.65	3.6 (0.17)	3.0	58	0.12
Ne	2.0	1.6 (0.50)	4.0	82	0.076
Ar	2.8	4.5 (0.68)	5.4	96	0.032
NH ₃	2.8	1.9 (0.66)	5.4	100	<0.02
N ₂	2.4	2.6 (0.56)	5.6	100	0.020
CH ₄	3.0	2.0 (0.75)	5.9	100	<0.02

^aCalculated density in g/l assuming ideal-gas law. The number density in cm⁻³ ($\times 10^{20}$) is given in parentheses.

^bThe charge density in e⁻/cm³ assuming valence electrons only.

^cFrom Table I.

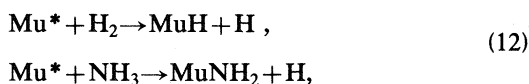
ed calculation employing Slater's definition⁴² of Z_{eff} does not change the following interpretation appreciably.) By and large it appears that electron density is the single most important criterion—high charge density (ρ_e) means large A_{abs} and hence short neutralization times. However, elastic and inelastic collision processes must also be important as evidenced by comparing A_{abs} for the different rare gases or in turn comparing these with polyatomic gases of comparable charge density. One would expect these effects to be most important near the low-energy asymptote of the charge-exchange regime. Thus, for example, of the rare gases at comparable ρ_e , He invariably exhibits the largest amplitude because it is most efficient at thermalization via elastic collisions. Even at a He pressure of only 1.2 atm, which corresponds to the lowest value of ρ_e in Table V, the muon amplitude is essentially the same as that in Xe or Kr at three times the charge density; compare also Ar and Xe. With the noble gases, there is no possibility for inelastic processes other than electronic excitation, which must surely have very small cross sections at these energies. In the case of polyatomic gases, however, both vibrational and rotational excitation are possible,³⁸ serving to moderate the muon more quickly. This effect has been alluded to previously and is also illustrated by the data in Table V. Thus, for example, in the case of N₂ and Ar at about the same ρ_e , it is found that N₂ always exhibits the higher amplitude. Similarly, H₂, with the second-lowest charge density

in Table V, exhibits a large amplitude, although in this case H₂ should also be an efficient elastic moderator. In this regard it is interesting to note that CH₄ seems to be relatively inefficient and the 100% amplitude seen at high pressure is probably mainly a charge-density effect (perhaps also with NH₃). These data require some detailed theoretical calculations, particularly in view of the fact that the kind of information displayed is not available in proton-charge-exchange studies.

C. Possible hot-atom processes in comparison with H-atom data

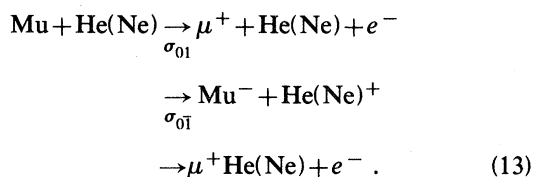
In comparing the relative muonium formation fractions in a given gas with the corresponding neutral fractions expected from proton charge exchange given in Table II, it should be kept in mind that the muon results are the final fractions at thermal energies whereas the proton results are extrapolated from higher energies assuming charge equilibration (Eq. 4). Nevertheless, qualitatively speaking, there is reasonably good agreement; certainly at least the trends are well reproduced. However, with the exception of Xe and Kr, there is less Mu seen in the present study than expected from proton charge exchange. This may indicate some inherent error in extrapolating available cross sections for proton charge exchange to the thermal energy regime and/or to a basic error in those cross sections themselves. On the other hand, particularly in the case

of the molecular gases, we can suspect hot-atom reactions, exemplified by



etc., which lead to a relative enhancement in the muon signal (a muon in any diamagnetic environment precesses essentially as a free μ^+).

What might the explanation be in the case of He and Ne, particularly in the case of He where there is really no Mu formed at all? There are a number of possibilities which could account for loss of Mu in these gases, following the charge-exchange regime, such as



At kinetic energies below 100 eV or so, the cross sections for the first two of these processes are only of order 10^{-18} cm² compared to typical elastic-scattering cross sections of order 10^{-15} cm². Nevertheless, there are a sufficient number of (elastic) collisions in the thermalization process, particularly in Ne, that one of these reactions may occur. This could again be considered as a type of hot-atom reaction. The last reaction, forming a molecular ion, may also occur. Certainly data on the *thermal* relaxation of the μ SR signal is strongly indicative of the presence of such molecular ions, but it does not reveal the mechanism for their production.^{13,21}

The energies at which one might expect hot-Mu abstraction or substitution reactions of the type represented by Eqs. (12) to be important are not well known. Since Mu formation itself begins at about 35 keV, hot reactions might also begin at these energies but it is unlikely that such reactions can be competitive with charge exchange and/or inelastic scattering during the charge-exchange regime. Thus it is most likely that epithermal (i.e., "hot") Mu reactions begin to occur with appreciable probability near the end of the charge-exchange regime, about 50 eV; the corresponding initial energy for hot-tritium (T) reactions would be about 1400 eV. The peak in such hot-atom cross sections, however, would probably occur below 10 eV since hot-tritium reactions (from nuclear recoil sources) are expected to show peaks in cross section in the 10-eV range⁴³ and, moreover, there is considerable mismatch between initial and final momenta for

Mu compared to tritium. This in turn suggests relatively small cross sections for hot-Mu compared to hot-T reactions. Such reactions do provide though a ready explanation for the reduced Mu fractions seen, particularly in the cases of H₂, NH₃, and CH₄, but it is difficult to arrive at a quantitative statement. The fact that for NH₃ and CH₄ there is less than 100% Mu found is regarded as particularly significant, since these cases are exothermic for Mu formation.

Traditionally, in liquid-phase muonium chemistry, epithermal or early time processes can be distinguished from *thermal* reaction rates by a measurement of the concentration or field dependence of the "residual" muon polarization.^{12,14,15,24} But charge exchange and hot-atom (or ion) reactions are both early time processes and hence their relative contributions to the experimental signal are not easily separated. It is, however, an interesting area for further study. Not only would the study of muonium hot-atom reactions in the gas phase be interesting in its own right, from the point of view of isotope effects on reactivity integrals,⁴⁴ but also an appreciation of the significance of these reactions is important towards resolving the current controversy of hot versus spur processes surrounding the interpretation of muonium formation in liquids.^{14,15,45}

TABLE VI. Absolute fractions (%) for muonium formation in gases compared with condensed media.

Target	Medium	f_{μ}^A	f_{Mu}^A	f_L	f_H
He	Gas ^a	100	0	0	15
	Liquid ^b	≥ 90	≤ 2	≤ 8	
Ar	Gas	26 ± 4	74 ± 4	0	85
	Liquid ^c	1.6 ± 1.0	97 ± 30	3 + 29	
	Solid	0.8 ± 0.2	91 ± 9	8 ± 9	
Kr	Gas	0 ± 5	100 ± 5	0	100
	Liquid	6.5 ± 0.1	57 ± 10	36 ± 10	
	Solid	1.4 ± 1.8	100 ± 10	0 ± 10	
Xe	Gas	0 ± 4	100 ± 4	0	100
	Liquid	3.3 ± 0.8	43 ± 9	54 ± 10	
	Solid	5.0 ± 3.3	79 ± 25	16 ± 28	
H ₂ O	Gas ^d	10 ± 5	90 ± 10	0	100
	Liquid ^e	62 ± 1	20 ± 1	18 ± 1	
	Solid	48 ± 1	52 ± 2	0	

^aGas-phase data from Table II, this paper.

^bFrom Crane *et al.*, Ref. 46.

^cAr, Kr, Xe condensed phases from Kiefl *et al.*, Ref. 40.

^dPreliminary data from TRIUMF, D. J. Arseneau *et al.*

^eH₂O condensed phases from Percival *et al.*, Ref. 14.

D. Comparison with other experiments

1. Muonium formation in condensed media

The fractions of muon and muonium found in the present gas-phase studies are compared with those similarly determined in condensed media in Table VI, for those cases in which both sets of data are available—the noble gases (except Ne) and also water. The fractions utilized in Table VI are the “absolute fractions” (f^A) which are commonly used in condensed media studies (and referred to as “polarizations”) and defined in terms of a 100% μ^+ signal in CCl_4 (or Al); hence $f_\mu^A + f_{\text{Mu}}^A \leq 1$. It is then the missing or “lost” fraction (f_L) which is of interest. The fractions f_H expected from proton charge exchange are also given for completeness. In gases, it is generally rather meaningless to talk about such missing fractions since, as demonstrated in Sec. IV B above, the absolute asymmetry A_{abs} and hence f_L is a strong function of the moderator pressure. Nevertheless it is conveniently introduced at this point for comparative purposes. The trend exhibited by the data in Table I and the assumption made in Table VI is that f_L (gas) \rightarrow zero in the limit of high pressure, which would be the expected result for condensed media (where the total slowing down times must be on the order of 1 ps). For the noble gases it can be seen that only in the case of He is there good agreement between the gas and condensed phases. In general, there is always a large missing fraction in the condensed phase, particularly in liquids. On the other hand, if the lost fraction represents depolarized Mu, as has been suggested at least in the case of water^{12,14} (which could *not* be

the result of the charge-exchange process), then, in fact, the initial Mu fractions are rather similar in the gas and condensed phases. It is to be noted that there appears to be two Mu components in both liquid Ar and solid Kr, one of which, particularly in liquid Ar, has a very fast relaxation.⁴⁰ In general, Mu relaxation rates are much faster in the condensed phase, presumably attributable to the dipole interaction of muonium with nuclear moments, an effect which is motionally averaged in the gas phase because of rapid Mu diffusion. However, these fast relaxations (up to $19 \mu\text{s}^{-1}$) introduce considerable error in the stated condensed-phase fractions, which must be kept in mind when comparing the results in Table VI. We are currently pursuing studies of Mu formation in different vapors in order to provide a detailed comparison with corresponding liquid-phase results.^{12,14,15,45}

2. Comparison with positronium formation

The positron and its positronium atom (e^+e^-) have at times been thought of as an analogous system to hydrogen⁴⁷ but the analogy is a poor one. The reduced mass of the positronium atom (Ps) is only half of the value in H or Mu and correspondingly the (gas-phase) ionization potential is only 6.8 eV. In no way can positronium be regarded as an isotope of hydrogen. It is nevertheless of some interest to compare the present results for Mu formation with those of Ps formation in the same gases. Positronium formation has been extensively studied in the noble gases,^{48,49} as well as in some molecular gases.⁵⁰ Data for the *total* fraction of Ps formed

TABLE VII. Positronium and Muonium formation fractions and Ore gap predictions in gases.

Gas	Ionization potential (eV) ^a	Positronium			Muonium			f_H^d
		f_{Ps}	f_{min}^b	f_{max}	f_{Mu}^c	f_{min}^b	f_{max}	
He	24.5	0.24 ^e	0.10	0.28	0	0.45	0.56	0.15
Ne	21.6	0.26	0.10	0.32	0.06±0.05	0.51	0.63	0.20
Ar	15.8	0.33	0.23	0.43	0.74±0.04	0.81	0.86	0.85
Kr	14.0	0.19	0.27	0.49	1.0 ±0.05	0.95	0.97	1.0
Xe	12.1	0.07	0.36	0.56	1.0 ±0.04	1.0	1.0	1.0
N ₂	15.6	0.34±0.02 ^f	0.43	0.44	0.84±0.04	0.60	0.87	0.90

^aThe ionization potential of the gas in eV.

^bOre gap predictions assuming a uniform energy distribution.

^cPresent data, Table II.

^dNeutral-H-atom fraction expected from proton charge exchange (Table II).

^ePs formation in rare gases from Coleman *et al.*, Ref. 48. No errors are given.

^fFrom Sharma and McNutt, Ref. 50.

(i.e., both ortho and para Ps) in the noble gases and in N_2 are compared with the corresponding muonium fractions in Table VII. The expected H-atom fractions from Table II are also given. A glance at this table reveals very large differences between the positronium (f_{Ps}) and muonium (f_{Mu}) fractions—Ps forms in all the rare gases, unlike Mu (or H) and in addition shows quite the opposite trends compared to Mu in those gases where both are found. Similarly in N_2 .

Positronium formation in a gas has traditionally been described in terms of the "Ore gap" model.^{47,48} In this model, for energies $E > E_I$, the ionization potential of the moderator, ionization and other inelastic cross sections are stated to be much larger than charge exchange so that Ps formation does not compete. Assuming a uniform energy distribution then, the maximum fraction of e^+ forming Ps is simply given by $f_{max} = 6.8/E_I$ (13.6 for Mu). The minimum fraction is determined by the position of the lowest electronic excited level of the gas, E_X , such that $f_{min} = (E_X - E_T)/E_X$ where E_T is the energy defect or threshold energy for Ps formation ($E_T = E_I - 6.8$ eV vs $E_I - 13.6$ eV for Mu). Hence Ps is expected to form in the gap between E_I and E_T with fractions in the range between f_{max} and f_{min} . These fractions for both Ps and Mu are also given in Table VII. In the case of Ps formation, f_{Ps} for He, Ne, and Ar is within the range predicted by the Ore model (which is the best that can be expected of it), but this model fails badly for Kr and particularly Xe. Some improvement for Kr is obtained if a uniform momentum distribution is used, but at the expense of worsening the agreement with the lower-mass gases.⁴⁸ It is curious to note that just the opposite prevails for Mu formation— f_{Mu} is within the (narrow) Ore limits for the heavier gases but these limits fail very badly for He and Ne, where something like 50% Mu formation is expected and essentially none is observed. The Ore model clearly has no general validity. The comparisons in Table VII simply reveal further that the muon and the proton exhibit an isotopic similarity in contradistinction to the positron. It would be interesting though to have some theoretical insight into the specific reasons for their differences.

V. CONCLUDING REMARKS

The positive muon in its thermalization process in the gas phase behaves similarly to the proton (but not the positron), as expected for isotopes where charge-exchange cross sections should be equal at equal velocities. Particularly in the polyatomic gases H_2 , NH_3 , and CH_4 there is relatively less muonium formed than expected from H-atom formation and correspondingly a larger diamagnetic muon signal, indicating the possibility of competing hot-atom reactions of the Mu atom. This is an interesting area for further study, not only for comparison with hot-tritium reactions but also as a guideline for understanding the origin of muonium fractions measured in condensed media.

A general feature of this work has been the observation that the experimental amplitude of the μ^+ SR or MSR signal is strongly pressure dependent, being larger at higher pressures and generally larger also in polyatomic gases. This can only be true if the time spent during the charge-exchange regime is comparable to the inverse of the hyperfine frequency, $1/\nu_0 = 0.22$ ns. Times for charge exchange of this order (at 1 atm pressure) mean that it is only the last one or two lowest-energy charge-exchange cycles (out of approximately 80) which ultimately determine the muonium formation fraction, not the energy at which the cross section peaks (~ 200 eV in a gas such as Ar). These times can be calculated but the cross sections for charge exchange in the low-energy regime are not well known. The present experiments represent the first direct measurements which could in turn be used to extract information on these cross sections.

ACKNOWLEDGMENTS

The continuing financial support of the Natural Sciences and Engineering Research Council of Canada is gratefully acknowledged (NSERC-IEP 17). We would also like to thank Dr. Masa Senba, of University of British Columbia, TRIUMF, and Dr. Bernie Shizgal, of Department of Chemistry, U.B.C., for their critical reading of the manuscript. This work is based on the Ph.D. thesis of R. J. M. at the University of British Columbia.

*Present address: Energy Mines and Resources, CANMET/ERL, Western Research Laboratory, P.O. Box 3294, Sherwood Park, Alberta T8A 2A6, Canada.

¹Proceedings of the Eleventh International Conference on the Physics of Electronic and Atomic Collisions, Kyoto,

1979, edited by N. Oda and K. Takayanagi (North-Holland, Amsterdam, 1980), p. 387.

²Phys. Scr. **23**, No. 2 (1981), edited by H. W. Drawin and K. Kotsonis.

³H. Tawara and A. Russek, Rev. Mod. Phys. **45**, 178

- (1973).
- ⁴H. Tawara, *At. Data Nucl. Data Tables* **22**, 491 (1978).
- ⁵B. H. Bransden, *Rep. Prog. Phys.* **35**, 949 (1972).
- ⁶R. A. Mapleton, *Theory of Charge Exchange* (Wiley-Interscience, New York, 1972).
- ⁷J. H. Newman *et al.*, Abstracts of papers, in *Proceedings of the Twelfth International Conference on the Physics of Electronic on Atomic Collisions*, Gatlinburg, Tennessee, 1981, Vol. 2, p. 615 (unpublished); J. H. Newman *et al.* (unpublished).
- ⁸D. L. Albritton, *At. Data Nucl. Data Tables* **22**, No.1 (1978).
- ⁹S. K. Allison, *Rev. Mod. Phys.* **30**, 1137 (1958).
- ¹⁰D. G. Fleming, D. M. Garner, and R. J. Mikula, *Hyperfine Interact.* **8**, 337 (1981).
- ¹¹D. M. Garner, Ph.D. thesis, University of British Columbia, 1979 (unpublished).
- ¹²P. W. Percival, *Radiochim. Acta* **26**, 1 (1979); D. C. Walker, *J. Phys. Chem.* **85**, 3960 (1981).
- ¹³R. J. Mikula, Ph.D. thesis, University of British Columbia, 1981 (unpublished).
- ¹⁴P. W. Percival, E. Roduner, and H. Fischer, *Chem. Phys.* **32**, 353 (1978); P. W. Percival, *Hyperfine Interact.* **6**, 373 (1979); **8**, 315 (1981); P. W. Percival, *J. Chem. Phys.*, **72**, 2900 (1980). See also Ref. 12.
- ¹⁵D. C. Walker, Y. C. Jean, and D. G. Fleming, *J. Chem. Phys.* **70**, 4534 (1979); **72**, 2909 (1980); D. C. Walker, *Hyperfine Interact.* **8**, 329 (1981).
- ¹⁶R. M. Mobley, Ph.D. thesis, Yale University, 1967 (unpublished); R. M. Mobley *et al.*, *J. Chem. Phys.* **44**, 4354 (1966); **47**, 3074 (1967).
- ¹⁷R. D. Stambaugh, Ph.D. thesis, Yale University, 1972 (unpublished); R. D. Stambaugh *et al.*, *Phys. Rev. Lett.* **33**, 568 (1974).
- ¹⁸B. A. Barnett *et al.*, *Phys. Rev. A* **11**, 39 (1975).
- ¹⁹A. E. Pifer, T. Bowen, and K. R. Kendall, *Nucl. Instrum. Methods* **135**, 39 (1976); C. J. Oram *et al.*, *ibid.* **179**, 95 (1981).
- ²⁰J. H. Brewer, *Hyperfine Interact.* **8**, 831 (1981).
- ²¹R. J. Mikula, D. G. Fleming, and D. M. Garner, *Hyperfine Interact.* **6**, 379 (1979).
- ²²D. G. Fleming, R. J. Mikula, and D. M. Garner, *Hyperfine Interact.* **8**, 307 (1981); **9**, 207 (1981).
- ²³A. M. Sachs and A. Sirlin, "Muon Decay" in *Muon Physics*, Vol. II, edited by V. W. Hughes and C. S. Wu (Academic, New York, 1975), p. 50.
- ²⁴D. G. Fleming *et al.*, *Adv. Chem. Ser.* **175**, 279 (1979).
- ²⁵J. H. Brewer *et al.*, *Muon Physics*, Vol. III, edited by C. S. Wu and V. W. Hughes (Academic, New York, 1975), p. 3.
- ²⁶A. Schenck, in *Nuclear and Particle Physics at Intermediate Energies*, edited by J. B. Warren (Plenum, New York, 1976), p. 159.
- ²⁷P. R. Bolton *et al.*, *Bull. Am. Phys. Soc.* **24**, 675 (1979).
- ²⁸D. G. Fleming, R. J. Mikula, and D. M. Garner, *J. Chem. Phys.* **72**, 2751 (1980); R. J. Mikula, D. M. Garner, and D. G. Fleming, *ibid.* **75**, 5362 (1981).
- ²⁹N. F. Mott and H. S. W. Massey, *Theory of Atomic Collisions*, 3rd edition (Clarendon, Oxford, 1965); J. B. Hasted, *Physics of Atomic Collisions* (Butterworths, London, 1964); H. S. W. Massey, *Electronic and Ionic Impact Phenomena*, (Oxford University Press, London, 1971), Vol. 3.
- ³⁰J. S. Briggs and K. Tallbjerg, *J. Phys. B* **12**, 2265 (1979).
- ³¹Dz. S. Belkic and R. K. Janev, *J. Phys. B* **6**, 2613 (1973).
- ³²V. Sidis, *J. Phys. B* **5**, 1517 (1972).
- ³³J. R. Macdonald, C. L. Cocke, and W. W. Eidson, *Phys. Rev. Lett.* **32**, 648 (1974); C. D. Lin and L. N. Tunnell, *J. Phys. B* **12**, L485 (1979).
- ³⁴C. D. Lin, S. C. Soong, and L. N. Tunnell, *Phys. Rev. A* **17**, 1646 (1978).
- ³⁵M. B. Shaw, J. Geddes, and H. B. Gilbody, *J. Phys. B* **13**, 4049 (1980); R. F. King and C. J. Latimer, *ibid.* **12**, 1477 (1979); B. M. Doughty, M. L. Goad, and R. W. Cernosek, *Phys. Rev. A* **18**, 29 (1978).
- ³⁶D. K. Brice, *Phys. Rev. A* **6**, 1791 (1972); W. Whaling, *Handb. Phys.* **34**, 193 (1958).
- ³⁷R. W. Bickes *et al.*, *Far. Disc. Chem. Soc.* **55**, 167 (1973); J. P. Toennies, *Physical Chemistry, an Advanced Treatise* edited by H. Eyring, D. Henderson, and W. Jost (Academic, New York, 1974), Vol. VI A, Chap. 5; G. O. Este, G. Knight, and G. Scoles, *Chem. Phys.* **35**, 421 (1978); N. Hishiruma, *Chem. Phys. Lett.* **70**, 361 (1980).
- ³⁸G. Bischof *et al.*, *J. Phys. B* **15**, 249 (1982); F. A. Gianturco, U. Gierz, and J. P. Toennies, *ibid.* **14**, 667 (1981); S. P. Kare and A. Kumar, *Physica (Utrecht)* **100C**, 135 (1980); A. K. Edwards *et al.*, *J. Chem. Phys.* **69**, 1985 (1978).
- ³⁹A. Mozumder, *J. Chem. Phys.* **72**, 6289 (1980).
- ⁴⁰R. F. Kiefl *et al.*, *J. Chem. Phys.* **74**, 308 (1981).
- ⁴¹K. W. Kehr, D. Richter, and G. Honig, *Hyperfine Interact.* **6**, 219 (1979); K. G. Petzinger, *ibid.* **8**, 639 (1981).
- ⁴²C. A. Coulson, *Valence* (Oxford University Press, London, 1961), pp. 39–40.
- ⁴³D. J. Malcolm-Lawes, *J. Chem. Soc. Faraday Trans. 2* **72**, 878 (1976); L. D. Spicer, *ibid.* **74**, 527 (1978); D. J. Malcolm-Lawes, *ibid.* **74**, 696 (1978); J. S. Wright, S. K. Gray, and R. N. Porter, *J. Phys. Chem.* **83**, 1033 (1979).
- ⁴⁴D. J. Malcolm-Lawes, *J. Chem. Soc. Faraday Trans. 2* **68**, 1613 (1972); **74**, 182 (1978); B. Shizgal, *J. Chem. Phys.* **74**, 1401 (1981), and references contained therein.
- ⁴⁵Y. Ito *et al.*, *Can. J. Chem.* **58**, 2395 (1980).
- ⁴⁶T. W. Crane *et al.*, *Phys. Rev. Lett.* **33**, 572 (1974).
- ⁴⁷V. I. Goldanskii, *At. Energy Rev.* **6**, 3 (1968); H. J. Ache, *Angew. Chem. Int. Ed. Engl.* **11**, 179 (1972).
- ⁴⁸C. Y. Leung and D. A. L. Paul, *J. Phys. B* **2**, 1278 (1969); P. G. Coleman *et al.*, *ibid.* **8**, L185 (1975).
- ⁴⁹M. Charlton *et al.*, *J. Phys. B* **12**, L633 (1979); **13**, L757 (1980).
- ⁵⁰J. D. McNutt, S. C. Sharma, and R. D. Brisbon, *Phys. Rev. A* **20**, 347 (1979); S. C. Sharma and J. C. McNutt, *Phys. Lett.* **73A**, 244 (1979).